High-precision mass measurements and production of neutron-deficient isotopes using heavy-ion beams at IGISOL

M. Vilén,[1, *] A. Kankainen,[1] P. Bączyk,[2] L. Canete,[1] J. Dobaczewski,[2, 3] T. Eronen,[1] S. Geldhof,[1]
A. Jokinen,[1] M. Konieczka,[2] J. Kostensalo,[1] I.D. Moore,[1] D.A. Nesterenko,[1] H. Penttilä,[1]
I. Pohjalainen,[1] M. Reponen,[1] S. Rinta-Antila,[1] A. de Roubin,[1] W. Satuła,[2] J. Suhonen,[1] and J. Äystö[1]

[1]*University of Jyväskylä, P.O. Box 35, FI-40014 University of Jyväskylä, Finland*
[2]*Institute of Theoretical Physics, Faculty of Physics,*
University of Warsaw, ul. Pasteura 5, PL-02-093 Warsaw, Poland
[3]*Department of Physics, University of York, Heslington, York YO10 5DD, United Kingdom*
(Dated: June 26, 2019)

An upgraded ion-guide system for the production of neutron-deficient isotopes with heavy-ion beams has been commissioned at the IGISOL facility with ^{36}Ar beam on ^{nat}Ni target. It was used together with the JYFLTRAP double Penning trap to measure the masses of ^{82}Zr, ^{84}Nb, ^{86}Mo, ^{88}Tc, ^{89}Ru ground states and the isomeric state ^{88}Tc^m. Of these, ^{89}Ru and ^{88}Tc^m were measured for the first time. The precisions of ^{82}Zr, ^{84}Nb and ^{88}Tc were significantly improved. The literature value for ^{86}Mo was verified. The measured states in ^{88}Tc were compared to shell-model calculations and additional constraints on the spins and level scheme were obtained. The masses of ^{82}Mo and ^{86}Ru have been predicted using the measured masses and theoretical mirror displacement energies, resulting in more tightly bound nuclei with smaller atomic mass uncertainties than reported in literature.

I. INTRODUCTION

Neutron-deficient nuclei in the mass region $A \approx 80 - 100$ provide invaluable data for understanding basic nuclear interactions. Being close to the $Z = N$ line, the protons and neutrons are filling the same orbitals, mainly the high spin $1g_{9/2}$ orbital above the subshell closure at $N = Z = 40$. This opens an interesting playground to investigate proton-neutron pairing [1, 2] as well as isospin symmetry [3, 4] in nuclei. Recent theoretical calculations for mirror (MDE) or triplet displacement energies (TDE) using extended Skyrme energy density functionals with proton–neutron-mixed densities and isospin-symmetry breaking terms have yielded a good agreement with experimental data in the lower mass region [3, 4]. For example, with next-to-leading order isospin-symmetry terms included, the root mean square deviation to experimental data for TDEs is only around 65 keV [4]. Above $A \approx 70$, the available experimental data for MDEs or TDEs is rather limited. There, these new calculations can provide predictions for the more exotic mirror partners in the isobaric doublets or triplets.

The neutron-deficient region close to $A \approx 80$ is known of shape coexistence and deformation. For example the $N = Z = 40$ nucleus ^{80}Zr is one of the most deformed nuclei known so far with a quadrupole deformation of $\beta_2 \approx 0.4$ [5]. Total-Routhian-surface calculations have indicated that the $g_{9/2}$ shell plays an important role in the shape evolution, with spherical, prolate, oblate and triaxial shapes predicted [6]. Even possible tetrahedral deformation has been proposed to exist in the region [7]. The onset of deformation is reflected in nuclear bind-

ing energies [8], and therefore new precision mass measurements can shed light on the shape changes in the $A = 80 - 100$ region.

The masses of neutron-deficient nuclei are also relevant for the astrophysical rapid proton (rp) capture process occurring in type I x-ray bursts [9, 10]. For reliable calculations of the produced light curves and burst ashes, the masses should be known with a precision of around 10 keV [9]. Previous mass measurements at JYFLTRAP [11–13] and SHIPTRAP [12, 14] have revealed large deviations up to 1 MeV to the earlier literature values. Before the Penning trap era, the masses were mainly based on beta-decay endpoint energies which are prone to underestimate the Q values, and hence the masses.

Neutron-deficient nuclei in the $A = 80 - 100$ region are rich of long-living isomeric states. Nucleons in the high spin $1g_{9/2}$ orbital can pair up from low to high spins, and odd nucleons can occupy also the low spin $2p_{1/2}$ orbital below, creating plenty of opportunities for spin-trap isomers. If a measured state is wrongly assigned as the ground state when in reality it is the isomer or a mixture of states, it can cause a substantial offset and lead to biased rp-process calculations. The excitation energies for low-lying, beta-decaying isomeric states have been very difficult to measure due to the lack of resolving power in available mass-measurement techniques. Recently, the phase-imaging ion cyclotron resonance (PI-ICR) technique [15] has made it possible to measure isomers at very low excitation energies ($E_x \geq 10$ keV), providing valuable data for understanding nucleon-nucleon interactions and single-particle properties in nuclei.

Many neutron-deficient nuclei in the $A = 80 - 100$ region have been challenging to produce at conventional ISOL facilities due to their refractory nature. One solution to the problem is the Ion Guide Isotope Separator On-Line (IGISOL) technique, which is a fast (sub-

ms) and chemically insensitive method to produce low-energy radioactive ion beams for nuclear physics experiments [16]. Although the IGISOL technique has proven to be a valuable tool in producing a great variety of rare isotope beams covering a large portion of the nuclear chart, heavy neutron-deficient nuclei lying further away from stability have been difficult to produce. The most commonly used ion guide types at IGISOL have been optimized for either light-ion induced fusion or proton-induced fission reactions [17]. There, the target foil is mounted in direct contact with the buffer gas and the primary beam traverses through the gas cell. For heavy ion beams this is not possible because the primary beam would create so much charge within the buffer gas that the overall efficiency would be substantially reduced due to the plasma effect. To tackle this problem, a heavy-ion ion guide (HIGISOL ion guide) [18–20] employing a shadow gas-cell method [21] was developed at IGISOL. In this method, the target is in front of the ion guide and the primary beam is stopped before entering the gas cell. The reaction products have large enough angles to bypass the beam dump and enter the gas cell. Recently, the HIGISOL ion guide was upgraded and used in an on-line experiment for the first time. In this article, we report on this commissioning experiment and precision mass measurements of neutron-deficient refractory isotopes improving the knowledge of the mass surface in the mass region $A \approx 80 - 90$.

II. EXPERIMENTAL METHODS

A. Production using the upgraded HIGISOL

The heavy neutron-deficient nuclei were produced employing $< 2.1 \, \mu$A, 222 MeV ^{36}Ar^{8+} beam impinging on a ^{nat}Ni target with a thickness of $4 \, \mu$m at the IGISOL facility [17, 23]. No fine-tuning of the primary beam energy was done with the degrader foils located on the upgraded HIGISOL platform (see FIG 1). The target was mounted on a rotating wheel located outside the gas cell next to the degrader foils. The primary beam was stopped right after the target wheel using a small cylindrical graphite beam dump mounted in front of the gas cell. This shielded the buffer gas from excessive ionization. The target was mounted on a rotating wheel and the degrader foils on frames that can be moved back and forth. These design choices allow the thermal power of the primary beam to be dissipated over a larger surface area. The electronics of the platform were totally renewed and a new control system was constructed utilizing a combination of a Raspberry Pi computer and an Arduino microcontroller. The rotational frequency of the target wheel as well as the position of the target wheel and degrader foils can now be remotely controlled using a Java-based software. Additionally, the whole platform can be remotely moved closer or further away from the gas cell, in parallel to the primary beam axis, based on
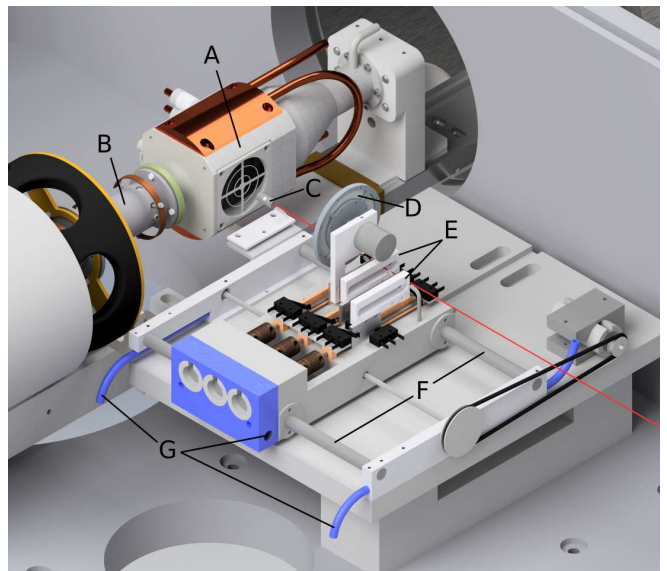

FIG. 1: The new HIGISOL system: A: Ion guide gas cell, B: SPIG [22], C: Beam dump, D: Target wheel, E: Degrader holder, F: Rails for distance adjustment, G: Coolant line
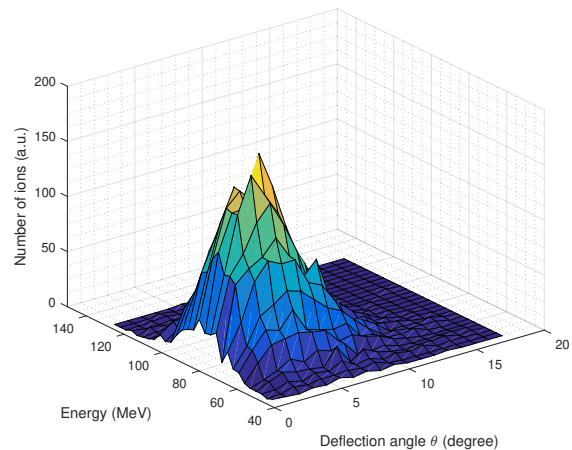

FIG. 2: Yield distribution (in arbitrary units) as a function of recoiling energy E_r and angle θ for 228.60 MeV ^{36}Ar beam on ^{nat}Ni target summed over all reaction products using the PACE4 program.

the position information provided by the system. This production method has been utilized at IGISOL in the past using two mechanical designs. For further details, the reader is referred to [19] for the original design and to [20] for the second iteration of the system design.

The choice of primary beam energy was made based on fusion-evaporation cross-section simulations using PACE4 [24], HIVAP [25] and NRV [26] codes. An example of an ion yield contour for ^{36}Ar^{8+} beam on a ^{nat}Ni target obtained with the PACE4 [24] code is presented in Fig. 2. The position of the yield maximum changes as a

function of primary beam energy in (E_r, θ) space, where E_r is the energy of recoiling reaction products and θ is the deflection angle. Reaction products have their yield maxima at slightly different, non-zero angles. Therefore, the distance between the gas cell and the target wheel needs to be optimized for each ion of interest so that the recoiling reaction products can enter the ion guide gas cell through its entrance window and are not implanted into the beam dump. In addition to the angle of the products, the kinetic energy of the reaction products has to be taken into account. Ions-of-interest must have enough energy after the target to go through the $2.17\,\mu$m-thick Havar window and then be stopped and thermalized within the buffer gas volume of the HIGISOL ion guide. Therefore, the pressure (stopping power) of the buffer gas needs to be adjusted so that the range of the ions does not exceed the inner diameter of the HIGISOL gas cell (approximately $6\,$cm). In order to accommodate different recoil energies and angular distributions resulting from the choice of primary beam energy and target, both the distance between the target and the gas cell, as well as buffer gas pressure, can be adjusted in the new system. These degrees of freedom are sufficient for optimizing the system for different primary beam energies for a variety reaction channels. In this experiment, the helium pressure was typically around 240 mbar.

Created reaction products captured in the ion guide gas cell were collected using a radio-frequency sextupole ion guide (SPIG) [22], with a typical charge-state being $q = +e$. The ions were accelerated to $30\,$keV and mass-separated using a dipole magnet before stopping, cooling and bunching in the radio-frequency quadrupole cooler-buncher (RFQ) [27]. The ion bunches from RFQ were injected into the double Penning trap mass spectrometer, JYFLTRAP [28].

B. Mass measurement techniques

Masses of the studied nuclides were measured utilizing Time-of-Flight Ion-Cyclotron Resonance (TOF-ICR) [29, 30] and Phase-Imaging Ion-Cyclotron Resonance (PI-ICR) [15] techniques. Measured ions were prepared in the purification trap via the mass-selective buffer gas cooling method [31] capable of providing isobarically purified ion samples. Masses were determined in the precision trap by measuring the ion's cyclotron frequency $\nu_c = qB/(2\pi m)$, where q and m are the charge and mass of the ion, respectively, and B is the magnetic field strength. The magnetic field strength was acquired by interleaving measurements of ions with well-known masses ($\nu_{c,ref}$) before and after each measurement of ion-of-interest (ν_c) and interpolating the field strength at the time of the ion-of-interest measurement. Identical excitation pattern was applied in the precision trap for the ion-of-interest and the reference ion in order to minimize the magnitude of any systematic errors due to different ion species. In this work, ^{85,87}Rb$^+$ ions were used as
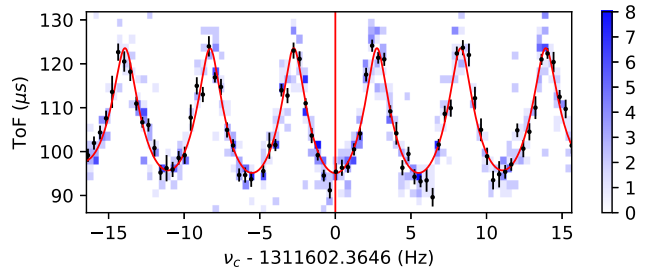

FIG. 3: Time-of-flight spectrum of ^{82}Zr$^+$. Background shading indicates the total number of ions.

references.

Two excitation schemes were utilized in the TOF-ICR measurements. A 200 ms quadrupole excitation pulse was used for ^{86}Mo and ^{88}Tc whereas the remaining masses were determined using the method of time-separated oscillatory fields [32, 33] with 25-750-25 ms (On-Off-On) excitation pattern for ^{84}Nb and 25-150-25 ms (On-Off-On) for ^{82}Zr and ^{89}Ru. For these cases, the position of the centre fringe was first verified via a measurement with a single conversion pulse. An example of a time-of-flight resonance of ^{82}Zr is presented in Fig. 3.

^{88}Tc was first measured using the TOF-ICR technique in order to improve the precision of the literature value of its ground-state mass. This measurement was followed by a PI-ICR measurement in which the energy separation between the ground state and presumed first isomeric state was measured. The mass difference between the two states is too low to result in two separate peaks using the TOF-ICR method.

In the PI-ICR measurements ion samples were prepared in the purification trap in the same way as with the TOF-ICR measurements. Ions were injected into the precision trap and the amplitude of residual magnetron and axial motion was damped using RF fields of suitable frequency and phase in preparation to the actual measurement. As ions are injected into the precision trap they acquire a non-zero amplitude for the magnetron and axial eigenmotions. If not addressed, the non-zero amplitudes would adversely affect measurement precision. Therefore, for each eigenmotion, a dipole pulse with a suitable amplitude π rad out of phase with the motion is applied in order to reduce the motion amplitude. The effect of the two eigenmotions can be seen as elongated spots on the MCP detector in the case of axial motion and incomplete conversions between ν_+ and ν_- eigenmotions in the case of the magnetron motion.

After the residual eigenmotion amplitudes were damped, a dipole excitation pulse at ν_+ frequency was applied followed by a phase accumulation time of 210 ms and a conversion pulse to convert the ion motion into magnetron motion. Finally, the ions were extracted onto a position sensitive delay line MCP detector. This measurement cycle was followed by one with slightly modified timings. The second cycle was identical to the first one

with the exception of the phase accumulation time being after the conversion pulse rather than before. Additionally, the center point of the precision trap was projected onto the detector. These three measurement cycles allowed us to calculate the mass difference between the ground and isomeric state of ^{88}Tc and ^{88}Tc^m. For a more detailed discussion on this mesurement technique the reader is referred to [15].

C. Data analysis

In the case of TOF-ICR method, the cyclotron frequency ν_c was measured multiple times for each nuclide. Each cyclotron frequency measurement was corrected, whenever possible, for shifts due to having multiple ions in the precision trap at the same time as described in [34]. Data available for ions of interest were not sufficient to allow for this kind of corrections to be made. However, all reference ion species were sufficiently abundant for applying the correction. Additionally, a correction due to B-field fluctuations, $\delta_B(\nu_{c,ref})/\nu_{c,ref} = \Delta t \cdot 8.18 \cdot 10^{-12}$ /min, was applied to each interpolated reference ion frequency, where Δt is the time between consecutive reference measurements, followed by calculation of frequency ratio (r) for each measurement. Atomic masses were calculated according to

$$r = \frac{\nu_{c,ref}}{\nu_c} = \frac{m}{m_{reference\ ion}} \qquad (1)$$

$$m = \frac{\nu_{c,ref}}{\nu_c} \cdot (m_{ref} - m_e) + m_e, \qquad (2)$$

where masses are expressed as atomic masses unless stated otherwise in subscripts. Electron binding energies were neglected as corrections beyond the precision of our measurements.

A weighted mean of frequency ratios along with internal and external errors [35] were calculated, and the larger one of the two was chosen as uncertainty of the mean. In most cases the Birge ratios were smaller than one, indicating that statistical uncertainties of individual measurements were conservative. Finally, a mass-dependent uncertainty $\delta_m(r)/r = \Delta m \cdot 2.2(6) \cdot 10^{-10}$ /u was added to the frequency ratio error, where Δm is the mass difference of the ion-of-interest and the reference ion. The applied data analysis process takes into account all systematic uncertainties that had been quantified at the time of the measurements. A detailed discussion on the different sources of systematic uncertainties at JYFLTRAP is to follow this article [36].

Data measured using the PI-ICR technique were used to determine the energy difference between the ground and the presumed first isomeric state of ^{88}Tc (see Fig. 4). The angle between final phases of magnetron and modified cyclotron motion was calculated from multiple measurements for both the ground and isomeric state, fol-
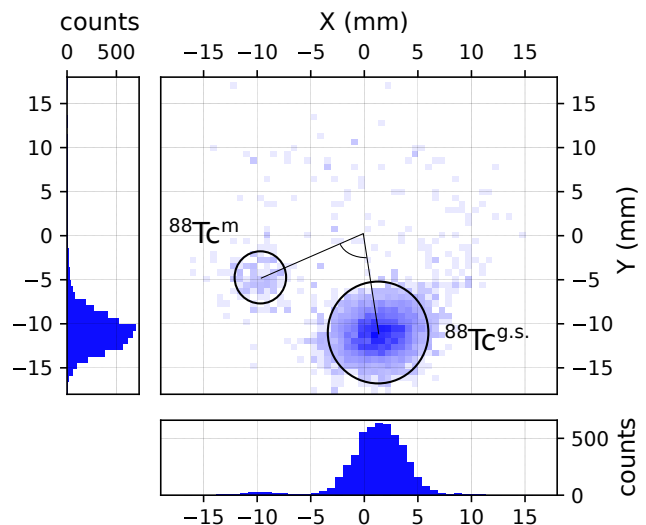

FIG. 4: ^{88}Tc ground state and isomeric state separated with the PI-ICR technique using 200 ms phase accumulation time.

lowed by the calculation of the cyclotron frequency using

$$\nu_c = \frac{\phi + 2\pi(n_+ + n_-)}{2\pi t}, \qquad (3)$$

where ϕ is the angle between final ν_+ and ν_- phases, n_+ and n_- the number of full revolutions ions completed in corresponding timing patterns within phase accumulation time t. A frequency ratio between the isomeric and ground state, $r = \nu_{c,\ gs}/\nu_{c,\ is}$, was calculated for each measurement. A weighted mean of the frequency ratios was used to determine the mass difference Δm between the two states, i.e. the excitation energy of the isomer E_x, using

$$E_x = \Delta m = (r - 1)(m_{gs} - m_e), \qquad (4)$$

where m_{gs} is the mass of the ground state determined in this work using the TOF-ICR technique. Inner and outer errors were determined, and the larger one was chosen as the error of the mean. Systematic uncertainties of the PI-ICR measurements with JYFLTRAP were studied in [37]. Systematic uncertainties discussed in [37] were found to be insignificant compared to the statistical uncertainty of this work.

One additional systematic uncertainty that was accounted for in this work is the shift of measured frequency as a function of the angle between spots accumulated on the detector in the PI-ICR method. As shown in Fig. 4, there was a non-zero angle between the isomeric and ground states. For the purpose of characterizing the effect of the angle another measurement was performed with stable ^{87}Rb ions where the ν_c frequency was determined using ^{87}Rb as a reference. Spot locations were tuned to match the ^{88}Tc measurement. In an ideal case a measurement like this would result in a frequency ratio

$r = 1$. However, the measurement resulted in

$$r - 1 = -3.7(2) \cdot 10^{-8}. \tag{5}$$

This systematic shift was corrected for in the results and, additionally, added quadratically as a systematic uncertainty. In the case of the PI-ICR measurement between ^{88}Tc and ^{88}Tc^m the effect of having multiple ion species in the measurement trap could not be accounted for due to low production rate of the isomeric state.

III. RESULTS AND DISCUSSION

A. Results and comparison to literature

In this work a total of six masses were measured: ^{82}Zr, ^{84}Nb, ^{86}Mo, ^{88}Tc, ^{88}Tc^m, and ^{89}Ru. Of these, ^{88}Tc^m and ^{89}Ru were measured for the first time. The mass-excess value for ^{89}Ru was found to be $-112(299)$ keV lower than the AME16 extrapolation. More detailed study of the mass surface and separation energies is presented in Sect. III C. The excitation energy of the isomeric state in ^{88}Tc^m was also determined for the first time and will be discussed in Sect. III B. Precisions for the masses of ^{82}Zr, ^{84}Nb, ^{86}Mo and ^{88}Tc, were significantly improved in this work. The resulting mass-excess values along with frequency ratios and literature values for the reference ions are presented in Table I.

The mass values determined for ^{86}Mo and ^{88}Tc in this work agree well with the previous literature values from Penning-trap measurements. The mass-excess value of ^{86}Mo, $-64109(3)$ keV, agrees almost perfectly with the SHIPTRAP Penning trap measurement $-64110(4)$ keV [14]. Also the mass excess value determined in this work for of ^{88}Tc, $-61669(2)$ keV, is in a good agreement with AME16. The AME16 value, $-61681(149)$ keV [38], is mainly based on an earlier measurement at JYFLTRAP [12] where the authors measured an unidentified state at $-61679.1(3.8)$ keV. The isomeric states could not be separated with the TOF-ICR technique used at that time, which lead the authors to assign the measured state as the high-spin ground state with an increased uncertainty of 87 keV based on analogy with neighboring odd-odd nuclide ^{90}Tc.

Of the studied nuclides, ^{82}Zr and ^{84}Nb have both been measured at the CSRe storage ring [40] using isochronous mass spectrometry, and were already included in AME16 [38] as private communications. Our more precise measurements suggest that ^{82}Zr is 17(12) keV and ^{84}Nb 25(13) keV less bound than in AME16, resulting in a disagreement of more than one sigma in both cases. Since the AME16 values were based on the CSRe storage ring measurements [40], we decided to do a more thorough comparison between the Penning-trap and storage-ring measurements to find out if there is a systematic deviation between the two methods.

Firstly, we gathered all published CSRe results and checked which nuclides had been measured also with a Penning trap. All in all, there were 17 nuclides available for the comparison with the CSRe publications [40–44]. These include publications on ^{37}K[45] and ^{39}Ca [46] from ISOLTRAP, ^{42}Ti [47], ^{45}V [48], ^{49}Mn [48], ^{52}Co [49], ^{52}Co^m [49], ^{53}Co [50], ^{55}Ni [50], ^{57}Cu [50], ^{59}Zn [50], ^{82}Zr (this work), ^{84}Nb (this work) from JYFLTRAP, ^{56}Cu [51] from LEBIT and ^{90}Ru [12, 52] from CPT, SHIPTRAP and JYFLTRAP. As can be seen from Fig. 5, Penning-trap measurements seem to give on the average around 20 keV higher mass values than CSRe. It is also noteworthy that only 4 out of 17 measurements give lower mass values than CSRe.

The obtained $\chi_n = \sqrt{\sum_i (ME_{trap,i} - ME_{CSRe,i})^2 / N}$ value between the two methods is $\chi_n = 1.54$ without the revised CSRe values for ^{45}V and ^{49}Mn [44], and $\chi_n = 1.47$ using the revised values. In both cases, the χ_n value is above the limit $\chi_n = 1 + 1/\sqrt{2N} = 1.18$. Therefore,the deviation between the trap and CSRe measurements cannot be explained solely by statistical fluctuations of the two datasets. Note that here only the JYFLTRAP measurement for ^{90}Ru was taken into account in order not to triple count the CSRe measurement for it.

In addition to the above mentioned measurements, estimations for ^{63}Ge, ^{65}As, ^{67}Se and ^{71}Kr can be obtained from the mirror displacement energies (MDE) and precise Penning-trap measurements of ^{63}Ga [53] at ISOLTRAP as well as ^{63}Ga [54], ^{65}Ge [54], ^{67}As [54] and ^{71}Br [55] at LEBIT. These are shown as open circles in Fig.5. Above A = 63, all the Penning-trap values are clearly higher than what the CSRe measurements yield.

B. Isomeric state in ^{88}Tc

In this work, we determined the excitation energy and the mass-excess value for the isomeric state in ^{88}Tc for the first time using the recently implemented PI-ICR technique at JYFLTRAP. Moreover, this enabled us to remove the uncertainty regarding the isomeric contamination, and therefore considerably improve the precision of the ground-state mass. The mass excess of ^{88}Tc^m was determined using a combination of two measurements. Firstly, the dominantly produced ground state was separated and measured using the TOF-ICR technique. Secondly, the less-populated isomeric state was successfully separated from the dominant state using the PI-ICR technique. The latter was used to measure the excitation energy of the isomeric state and to determine the relative abundance of the two states. It was found that the ground state accounted for 97(1) % of ions detected after the Penning traps. The excitation energy of the isomeric state was measured to be 70.4(31) keV.

Based on the yield ratio and the excitation energy of the isomeric state, i.e. frequency ratio of the two states, a correction was made for the TOF-ICR measurement of ^{88}Tc to account for the presence of the weakly populated isomeric state. The applied correction was calculated

TABLE I: Frequency ratios (r) and mass-excess values (ME) determined in this work with JYFLTRAP and compared with AME16 [38]. All measurements were done with singly-charged ions. The reference masses, ^{85}Rb($ME = -82167.331(5)$[38]) and ^{87}Rb ($ME = -84597.791(6)$[38]) were adopted from AME16, and # signs indicate extrapolated values therein. The excitation energy for ^{88}Tc^m, $E_x = 70.4(31)$ keV, was determined for the first time using the PI-ICR technique, see text for details.

Nuclide	Reference	$r = \nu_{c,ref}/\nu_c$	ME_{JYFL}(keV)	ME_{AME16}(keV)	$\Delta ME_{JYFL-AME16}$(keV)
^{82}Zr	^{85}Rb	0.964 903 56(2)	$-63613(2)$	$-63631(12)$	17(12)
^{84}Nb	^{85}Rb	0.988 488 167(5)	$-61193.8(4)$	$-61219(13)$	25(13)
^{86}Mo	^{85}Rb	1.012 005 28(6)	$-64112(5)$	$-64113(5)$	$-2(6)$
^{88}Tc	^{87}Rb	1.011 789 55(5)	$-61670(4)$	$-61681(149)$	11(149)
^{88}Tc^{ma}	^{88}Tc	1.000 000 86(4)	$-61600(5)$	$-61680(340)\#$ [39]	$-80(340)\#$
^{89}Ru	^{85}Rb	1.047 408 9(3)	$-58372(21)$	$-58260(298)\#$	$-112(299)\#$

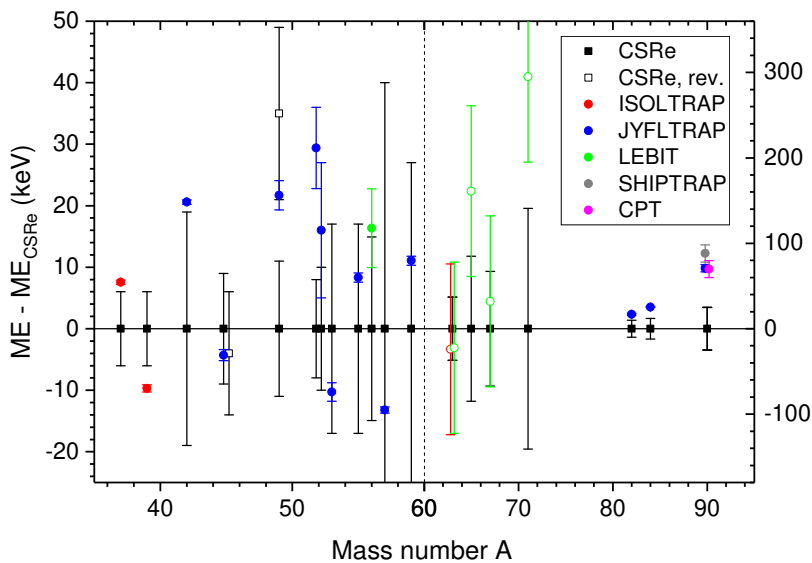^{a} Measured using the PI-ICR technique.

FIG. 5: Comparison of Penning-trap measurements performed at ISOLTRAP, JYFLTRAP, LEBIT, SHIPTRAP and CPT to the results from CSRe. The open circles denote the masses estimated based on the masses of ^{63}Ga, ^{65}Ge, ^{67}As and ^{71}Br and mirror displacement energies. The revised CSRe values for ^{45}V and ^{49}Mn are shown by an open square. Note the different y-axis scale after A = 60 (shown on the righ-hand side).

using

$$\nu_{c,measured} = a\nu_{c,gs} + (1-a)\nu_{c,is}, \quad (6)$$

leading to

$$\frac{\nu_{c,measured}}{\nu_{c,gs}} = a + (1-a)\frac{\nu_{c,is}}{\nu_{c,gs}}, \quad (7)$$

where a is the fraction of ions in the ground state. Using frequency ratio $\nu_{c,is}/\nu_{c,gs}$ from the PI-ICR measurement, we get

$$\nu_{c,measured} = (1 - 25.7 \cdot 10^{-9})\nu_{c,gs}. \quad (8)$$

Applying this correction to all TOF-ICR measurements of ^{88}Tc resulted in a shift of -2.1 keV to the ground-state

mass excess. In order to be conservative with our results, the error of the ground-state mass excess was increased by the same amount. The mass excess and frequency ratio values of ^{88}Tc and ^{88}Tc^m presented in Table I have this correction included.

In addition to the states measured in this work, there is a second isomeric state with a very short half-life, $T_{1/2} = 146$ ns, listed in the latest NUBASE16 evaluation of nuclear properties [39]. The half-life of the state is several orders of magnitude below what is reachable via Penning-trap mass measurements. Therefore, we conclude that our results correspond to states listed as the ground state and the longer-lived isomeric state in [39], with half-lives 6.4 s and 5.8 s, respectively.

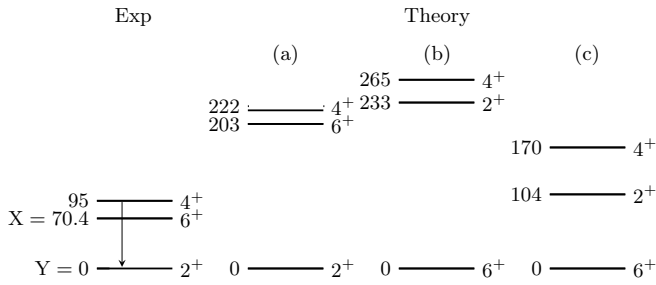The order of the three lowest states in ^{88}Tc has re-

FIG. 6: Experimental and theoretical excitation energies of ^{88}Tc using $1p_{1/2}-0g_{9/2}$ model space. Interactions used were (a) slgt0 [56] (b) jun45 [57] and (c) jj44b [58].
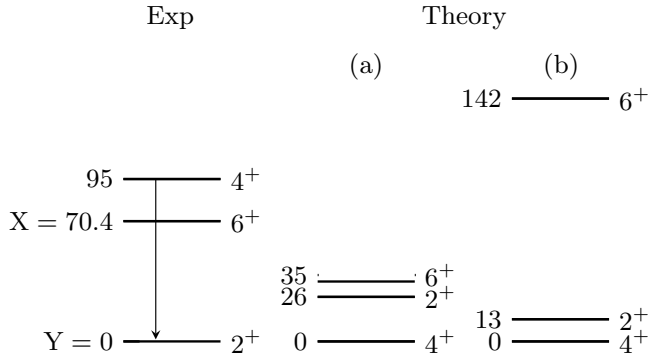

FIG. 7: Experimental and theoretical excitation energies of ^{88}Tc using $0f_{5/2}-1p-0g_{9/2}$ model space. Interactions used were (a) jun45 [57] and (b) jj44b [58].

mained unclear. The presumed ground state of ^{88}Tc was observed for the first time in 1991, and assigned as $7, 8^+$ due to observed feeding 8^+ and 7^- states in ^{88}Mo [59]. The beta-decay study of Odahara et al.[60] suggested spins of 3^+ and 6^+ for the detected states with half-lives of 5.8(2) s and 6.4(8) s, respectively. The isomeric states of ^{88}Tc were further studied by Garnsworthy et al. [61]. Based on the observed 95-kev transition, which they assign tentatively as $4^+ \to 2^+$, and by comparing with the shell-model calculations using the Gross-Frenkel interaction [62] in a $1g_{9/2} - 2p_{1/2}$ model space, they suggest that the $(5^+, 6^+, 7^+)$ state listed as the ground state in [39] would in reality be the first isomeric state with spin 6^+. The ground state would then be 2^+ fed by the observed 95-keV transition.

The excitation energy measured in this work, $E_x = 70.4(31)$ keV, is higher than the observed 95 keV transition energy for $4^+ \to 2^+$ or $2^+ \to 4^+$ in [61]. Therefore, either the 4^+ or 2^+ state should lie above the isomeric state observed in this work. We studied possible options for the order of the states: (i) 6^+ ($E_x = 0$ keV), 2^+ ($E_x = 70$ keV), 4^+ ($E_x = 165$ keV), (ii) 6^+ ($E_x = 0$ keV), 4^+ ($E_x = 70$ keV), 2^+ ($E_x = 165$ keV), (iii) 2^+ ($E_x = 0$ keV), 6^+($E_x = 70$ keV), 4^+ ($E_x = 95$ keV), or (iv) 4^+($E_x = 0$ keV), 6^+($E_x = 70$ keV), 2^+($E_x = 95$ keV). We

calculated half-lives for the isomeric states using Weisskopf estimates. The option (i) is not plausible since the 165-keV $E2$ transition from 4^+ to 6^+ should be faster and more intense than the 95-keV transition observed clearly in [61], and therefore should have been detected in the earlier works [59, 61]. The fact that no other gamma rays than the 95-keV transition was observed from the 146(12)-ns isomeric state in [61] is revealing: the energy difference between the states has to be so small that it was below the detection threshold in [61].

For option (ii), the 70-keV $E2$ transition would be too fast for the state being a beta-decaying isomer detected with a Penning trap. The same is true for option (iv), and it can be excluded. Therefore, the most likely option is (iii), with 2^+ as the ground state and 6^+ as the isomeric state just below the 4^+ state (see Figs. 6 and 7). This result is somewhat surprising because 97(1) % of the ions detected after the Penning traps belonged to the ground state. Heavy-ion fusion evaporation reactions tend to predominantly populate higher-spin states. As such, the production ratio of the states would favor 6^+ as the ground state, i.e. option (i). Note that the half-lives of the ground and isomeric states are roughly similar [60] and long compared to the trap cycles, and cannot therefore explain the dominance of the ground-state ions.

Shell-model calculations were performed in order to compare our experimental results with theoretical models. Three nuclear interactions were employed, slgt0 [56], jun45 [57] and jj44b [58], using the same model space as in [61], $1p_{1/2}-0g_{9/2}$. Acquired level schemes, presented in Fig. 6, do not give a consistent picture of the order of the states and, additionally, significantly overestimate excitation energies. It is interesting to note, however, that jj44b in the smaller model space (Fig. 6.(c)) would agree well with the level ordering of option (i), i.e. 6^+ ground state and 2^+ isomer. This would also be compatible with the production argument that higher-spin states are favored in heavy-ion fusion evaporation reactions.

Shell model calculations were repeated using a larger model space, $0f_{5/2}-1p-0g_{9/2}$, with jun45 and jj44b interactions, see Fig. 7. The larger model space changed the order of the states as well as produced energy levels closer to experimental results. However, spins of the states are still not in agreement with expectations based on experimental results. Discrepancies between the experimental and theoretical level schemes, as well as between the levels schemes obtained with different theoretical model spaces, show that theoretical approaches for this particular nuclide are highly sensitive and cannot offer additional support for the spin assignments. All theoretical calculations, however, predict 2^+, 4^+ and 6^+ to be among the three lowest states.

C. Mass surface in the region

The effect of this work on the mass surface was studied via two-neutron (S_{2n}) and two-proton (S_{2p}) separation

energies, and neutron pairing-gap energies D_n. Two-neutron and two-proton separation energies are sensitive to trends in nuclear structure irrespective of odd-even staggering, making them a useful tool in searching for changes in nuclear deformation and onset of shell-closures. Neutron pairing gap energies D_n were used as a complimentary tool to S_{2n} and S_{2p} energies since it is a quantity highly sensitive to pairing of single neutrons.

Two-neutron separation energies in the region of this work are presented in Fig. 8. The new data introduces minor changes to Zr, Nb, Mo and Tc isotopic chains. The new values offer improved precision compared to [38] and follow the trend set by the literature values. This work extends the Ru isotopic chain by one isotope, revealing an over-estimation of S_{2n} energy by extrapolated theoretical values.

Two-proton separation energies S_{2p}, see Fig. 9, largely mirror the changes seen in two-neutron separation energies. Similarly as with the S_{2n} values, minor changes are introduced to Zr, Nb, Mo and Tc isotopic chains by the new results. Also, Ru chain is again extended by one additional isotope, revealing an under-estimation of S_{2p} energy by extrapolated theoretical values.

The new S_{2n} and S_{2p} results suggest minor changes compared to theoretical values in the case of the Ru chain, but do not reveal any major changes in the case of previously experimentally-known masses.

Neutron pairing-gap energies

$$D_n = (-1)^{N+1}[S_n(Z, N+1) - S_n(Z, N)] \qquad (9)$$

[63], where S_n are neutron separation energies, were also studied. D_n energies, contrary to S_{2n} and S_{2p}, are an effective indicator of changes in pairing of individual valence neutrons. This is highlighted by the fact that the neutron pairing gap energy can be expressed using the empirical neutron pairing gap $\Delta^3(N) = D_n(N)/2$ which is also known as the odd-even staggering parameter [64]. Neutron pairing gap energies affected by this work are presented in Fig. 10.

Similarly to S_{2n} and S_{2p} energies, the neutron pairing gap energies of this work produce only minor changes in Zr, Nb, Mo and Tc isotopic chains. In the case of ^{90}Ru, this work shows a clear over-estimation of odd-even staggering by extrapolated values of [38].

D. Mass predictions using mirror displacement energies

In this work, we measured the ground-state mass of ^{89}Ru for the first time. Our result, $-58372(21)\,\text{keV}$, indicated that it is somewhat (by $-112(299)\,\text{keV}$) more bound than the extrapolated literature value, $-58260(298)\,\text{keV}$ [38]. Since we measured many isospin projection $T_Z = (N - Z)/2 = +1$ nuclei, we decided to investigate what kind of mass predictions we obtain for the $T_Z = -1$ mirror partners by combining our precise mass measurements of $T_Z = +1$ nuclei with the
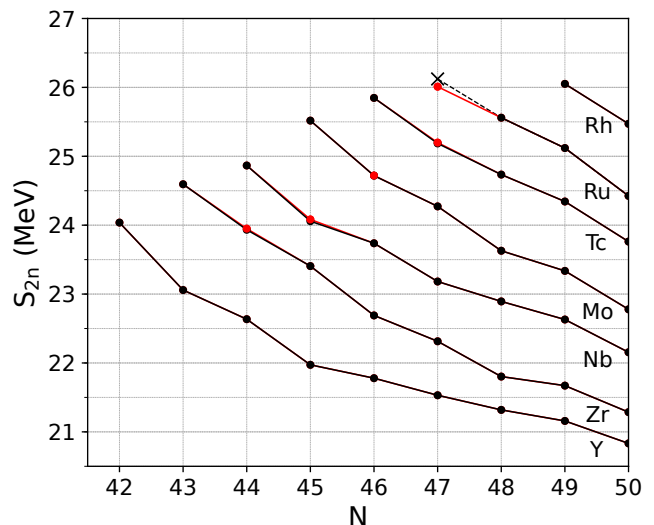

FIG. 8: Two-neutron separation energies S_{2n}. Experimental AME16 [38] values are presented with black dots and results affected by this work with red dots. An extrapolated value for ^{91}Ru adopted from [38] is presented with an X.
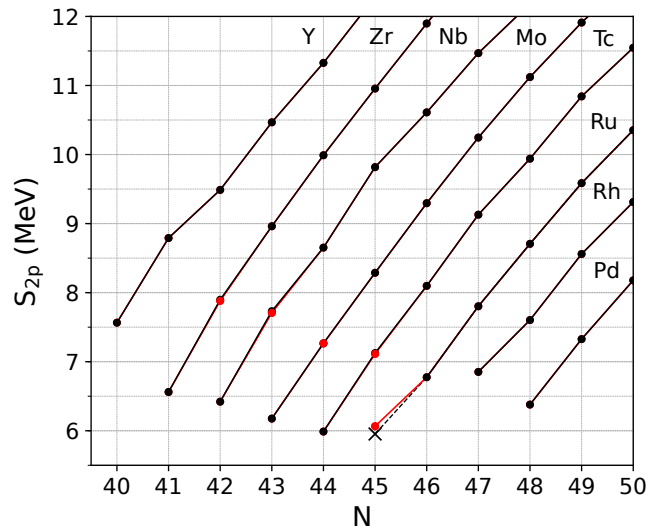

FIG. 9: Two-proton separation energies S_{2p}. Experimental AME16 [38] values are presented with black dots and results affected by this work with red dots. An extrapolated value for ^{89}Ru adopted from [38] is presented with an X.

state-of-the-art theoretical calculations for mirror displacement energies (MDE) [3, 4]. The theoretical calculations employ extended Skyrme energy density functionals with proton–neutron-mixed densities and isospin-symmetry breaking terms in next-to-leading-order. The agreement with these calculations with the experimental energies at lower mass numbers, such as $A = 52$, has

TABLE II: Mass-excess values (ME) determined in this work using theoretical MDEs [?] compared with AME16 [38], where # indicates extrapolated values therein.

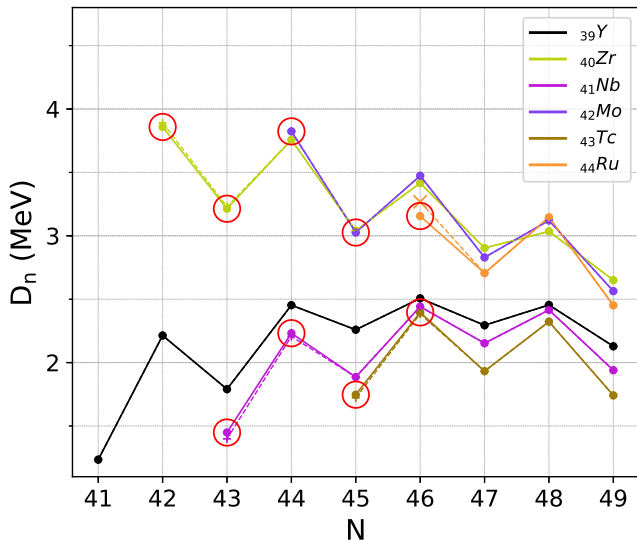| Nuclide	T_z	MDE(keV)	ME_{JYFL}(keV)	ME_{AME16}(keV)	$\Delta ME_{JYFL-AME16}$(keV)
^{86}Ru	-1	25370(50)(180)	-40310(190)	-39770(400)#	-540(450)
^{82}Mo	-1	24290(50)(180)	-40910(190)	-40370(400)#	-540(450)

FIG. 10: Pairing-gap energies D_n. Experimental AME16 [38] values are presented with dashed lines and AME16 values together with results from this work with solid lines. An extrapolated value for ^{90}Ru adopted from [38] is presented with an X. Results affected by this work are highlighted with red circles.

been excellent [4].

The calculations yield mirror displacement energies of 24290(50)(180) keV for A = 82 and 25370(50)(180) keV for A = 86. Predictions for $A = 84$ and $A = 88$ were not possible due to unbound $T_Z = -1$ partners. The mass excesses of $T_Z = -1$ isotopes ^{86}Ru and ^{82}Mo were calculated utilizing the results from this work for respective $T_z = +1$ mirror nuclei ^{86}Mo and ^{82}Zr (see Table II.). The results from this work consistently predict more bound nuclei than literature [38], and also decrease the uncertainty of the predicted mass-excess values.

IV. CONCLUSIONS

An upgraded system for the production of neutron-deficient isotopes using heavy-ion beams has been successfully commissioned at IGISOL. The new system was used in its first on-line experiment where a total of six masses were measured, ^{82}Zr, ^{84}Nb, ^{86}Mo, ^{88}Tc, ^{88}Tc^m and ^{89}Ru. The precisions of ^{82}Zr, ^{84}Nb and ^{88}Tc were improved and the literature value of ^{86}Mo was verified.

^{88}Tc^m and ^{89}Ru were measured for the first time.

The new results for ^{82}Zr and ^{84}Nb do not fully agree with the literature values based on the measurements at the CSRe storage ring in Lanzhou [40]. A thorough comparison between the results from the CSRe and several Penning traps was performed, and a deviation larger than what can be explained by statistical fluctuations alone was discovered. The comparison suggests that Penning trap measurement seem to produce on average about 20 keV higher mass values. The impact on the astrophysical rp-process was already studied in [40]. A systematic shift of around 10 keV will not have a huge impact on the calculated abundances and light curves as it will be partly cancelled out in the proton separation energies used as an input for the rp-process calculations.

The excitation energy for the long-living isomer in ^{88}Tc, 70.4(31) keV, was determined for the first time in this work. The order of the lowest three levels in ^{88}Tc was studied based on the excitation energy together with known and expected half-lives for the states. Based on the new limitations, 2^+ is most likely the ground state and 6^+ the first isomer in ^{88}Tc. This is somewhat unexpected since the ground state was dominantly produced, contrary to the expectation of better production for the higher-spin state.

Masses of ^{82}Zr and ^{86}Mo measured in this campaign were used to study corresponding mirror nuclei ^{82}Mo and ^{86}Ru via theoretical MDE's. The resulting mass-excess values are more precise than predicted in the most recent atomic mass evaluation for ^{82}Mo and ^{86}Ru [38]. The new values suggest that the studied nuclei are more tightly bound than expected from extrapolations of the mass surface [38]. This is consistent with the observation that the mass of ^{89}Ru measured in this work for the first time was lower than the AME16 extrapolation.

In conclusion, we have improved the knowledge of the mass surface in the neutron-deficient mass region $A = 82 - 89$ by precise Penning-trap measurements. The results indicate that the extrapolated masses might be somewhat overpredicted in this region. Future precision measurements aiming toward $N = Z$ nuclei or beyond, are anticipated to shed more light on the evolution of the mass surface in this region rich of isomeric states and structural changes. The recently commissioned PI-ICR technique will be an invaluable tool for revealing and identifying longer-living isomeric states as demonstrated with ^{88}Tc in this work.

ACKNOWLEDGMENTS

————————————————

[1] B. Cederwall, F. G. Moradi, T. Bäck, A. Johnson, J. Blomqvist, E. Clément, G. de France, R. Wadsworth, K. Andgren, K. Lagergren, A. Dijon, G. Jaworski, R. Liotta, C. Qi, B. M. Nyakó, J. Nyberg, M. Palacz, H. Al-Azri, A. Algora, G. de Angelis, A. Ataç, S. Bhattacharyya, T. Brock, J. R. Brown, P. Davies, A. D. Nitto, Z. Dombrádi, A. Gadea, J. Gál, B. Hadinia, F. Johnston-Theasby, P. Joshi, K. Juhász, R. Julin, A. Jungclaus, G. Kalinka, S. O. Kara, A. Khaplanov, J. Kownacki, G. L. Rana, S. M. Lenzi, J. Molnár, R. Moro, D. R. Napoli, B. S. N. Singh, A. Persson, F. Recchia, M. Sandzelius, J.-N. Scheurer, G. Sletten, D. Sohler, P.-A. Söderström, M. J. Taylor, J. Timár, J. J. Valiente-Dobón, E. Vardaci, and S. Williams, Nature 469, 68 (2011).
[2] Progr. Part. Nucl. Phys. 78, 24 (2014).
[3] P. Bączyk, J. Dobaczewski, M. Konieczka, W. Satuła, T. Nakatsukasa, and K. Sato, Phys. Lett. B 778, 178 (2018).
[4] P. Bączyk, W. Satuła, J. Dobaczewski, and M. Konieczka, Journal of Physics G: Nuclear and Particle Physics 46, 03LT01 (2019).
[5] C. J. Lister, M. Campbell, A. A. Chishti, W. Gelletly, L. Goettig, R. Moscrop, B. J. Varley, A. N. James, T. Morrison, H. G. Price, J. Simpson, K. Connel, and O. Skeppstedt, Phys. Rev. Lett. 59, 1270 (1987).
[6] S. J. Zheng, F. R. Xu, S. F. Shen, H. L. Liu, R. Wyss, and Y. P. Yan, Phys. Rev. C 90, 064309 (2014).
[7] J. Dudek, A. Góźdź, N. Schunck, and M. Miśkiewicz, Phys. Rev. Lett. 88, 252502 (2002).
[8] D. Lunney, J. M. Pearson, and C. Thibault, Rev. Mod. Phys. 75, 1021 (2003).
[9] H. Schatz, Int. J. Mass Spectrom. 251, 293 (2006), uLTRA-ACCURATE MASS SPECTROMETRY AND RELATED TOPICS Dedicated to H.-J. Kluge on the occasion of his 65th birthday anniversary.
[10] H. Schatz and W.-J. Ong, Astrophys. J. 844, 139 (2017).
[11] A. Kankainen, S. A. Eliseev, T. Eronen, S. P. Fox, U. Hager, J. Hakala, W. Huang, J. Huikari, D. Jenkins, A. Jokinen, S. Kopecky, I. Moore, A. Nieminen, Y. N. Novikov, H. Penttilä, A. V. Popov, S. Rinta-Antila, H. Schatz, D. M. Seliverstov, G. K. Vorobjev, Y. Wang, and J. Äystö, in The 4th International Conference on Exotic Nuclei and Atomic Masses, edited by C. J. Gross, W. Nazarewicz, and K. P. Rykaczewski (Springer Berlin Heidelberg, Berlin, Heidelberg, 2005) pp. 129–130.
[12] C. Weber, V.-V. Elomaa, R. Ferrer, C. Fröhlich, D. Ackermann, J. Äystö, G. Audi, L. Batist, K. Blaum, M. Block, A. Chaudhuri, M. Dworschak, S. Eliseev, T. Eronen, U. Hager, J. Hakala, F. Herfurth, F. P. Heßberger, S. Hofmann, A. Jokinen, A. Kankainen, H.-J. Kluge, K. Langanke, A. Martín, G. Martínez-Pinedo, M. Mazzocco, I. D. Moore, J. B. Neumayr, Y. N. Novikov, H. Penttilä, W. R. Plaß, A. V. Popov, S. Rahaman, T. Rauscher, C. Rauth, J. Rissanen, D. Rodríguez, A. Saastamoinen, C. Scheidenberger, L. Schweikhard, D. M. Seliverstov, T. Sonoda, F.-K. Thielemann, P. G. Thirolf, and G. K. Vorobjev, Phys. Rev. C 78, 054310 (2008).
[13] V.-V. Elomaa, G. K. Vorobjev, A. Kankainen, L. Batist, S. Eliseev, T. Eronen, J. Hakala, A. Jokinen, I. D. Moore, Y. N. Novikov, H. Penttilä, A. Popov, S. Rahaman, J. Rissanen, A. Saastamoinen, H. Schatz, D. M. Seliverstov, C. Weber, and J. Äystö, Phys. Rev. Lett. 102, 252501 (2009).
[14] E. Haettner, D. Ackermann, G. Audi, K. Blaum, M. Block, S. Eliseev, T. Fleckenstein, F. Herfurth, F. P. Heßberger, S. Hofmann, J. Ketelaer, J. Ketter, H.-J. Kluge, G. Marx, M. Mazzocco, Y. N. Novikov, W. R. Plaß, S. Rahaman, T. Rauscher, D. Rodríguez, H. Schatz, C. Scheidenberger, L. Schweikhard, B. Sun, P. G. Thirolf, G. Vorobjev, M. Wang, and C. Weber, Phys. Rev. Lett. 106, 122501 (2011).
[15] S. Eliseev, K. Blaum, M. Block, A. Dörr, C. Droese, T. Eronen, M. Goncharov, M. Höcker, J. Ketter, E. M. Ramirez, D. A. Nesterenko, Y. N. Novikov, and L. Schweikhard, Applied Physics B 114, 107 (2014).
[16] J. Ärje, J. Äystö, H. Hyvönen, P. Taskinen, V. Koponen, J. Honkanen, A. Hautojärvi, and K. Vierinen, Phys. Rev. Lett. 54, 99 (1985).
[17] J. Äystö, Nuclear Physics A 693, 477 (2001).
[18] I. D. Moore, P. Dendooven, and J. Ärje, Hyperfine Interactions 223, 17 (2013).
[19] J. Huikari, P. Dendooven, A. Jokinen, A. Nieminen, H. Penttilä, K. Peräjärvi, A. Popov, S. Rinta-Antila, and J. Äystö, Nuclear Instruments and Methods in Physics Research Section B: Beam Interactions with Materials and Atoms 222, 632 (2004).
[20] V.-V. Elomaa, Mass measurements for explosive nucleosynthesis in stars, Ph.D. thesis, University of Jyväskylä (2009).
[21] R. Béraud, A. Emsallem, A. Astier, R. Bouvier, R. Duffait, Y. L. Coz, S. Morier, A. Wojtasiewicz, Y. Lazarev, I. Shirokovsky, I. Izosimov, D. Barnéoud, J. Genevey, A. Gizon, R. Guglielmini, G. Margotton, and J. Vieux-Rochaz, Nuclear Instruments and Methods in Physics Research Section A: Accelerators, Spectrometers, Detectors and Associated Equipment 346, 196 (1994).
[22] P. Karvonen, I. Moore, T. Sonoda, T. Kessler, H. Penttilä, K. Peräjärvi, P. Ronkanen, and J. Äystö, Nuclear Instruments and Methods in Physics Research Section B: Beam Interactions with Materials and Atoms 266, 4794 (2008).
[23] I. Moore, T. Eronen, D. Gorelov, J. Hakala, A. Joki-

nen, A. Kankainen, V. Kolhinen, J. Koponen, H. Penttilä, I. Pohjalainen, M. Reponen, J. Rissanen, A. Saastamoinen, S. Rinta-Antila, V. Sonnenschein, and J. Äystö, Nuclear Instruments and Methods in Physics Research Section B: Beam Interactions with Materials and Atoms **317**, 208 (2013).

[24] O. Tarasov and D. Bazin, Nuclear Instruments and Methods in Physics Research Section B: Beam Interactions with Materials and Atoms **266**, 4657 (2008).

[25] N. Wang and W. Scheid, Physical Review C **78** (2008), 10.1103/physrevc.78.014607.

[26] V. I. Zagrebaev, A. S. Denikin, A. V. Karpov, A. P. Alekseev, M. A. Naumenko, V. A. Rachkov, V. V. Samarin, and V. V. Saiko, "NRV web knowledge base on low-energy nuclear physics," (1999).

[27] A. Nieminen, J. Huikari, A. Jokinen, J. Äystö, P. Campbell, and E. Cochrane, Nuclear Instruments and Methods in Physics Research Section A: Accelerators, Spectrometers, Detectors and Associated Equipment **469**, 244 (2001).

[28] T. Eronen, V. S. Kolhinen, V. V. Elomaa, D. Gorelov, U. Hager, J. Hakala, A. Jokinen, A. Kankainen, P. Karvonen, S. Kopecky, I. D. Moore, H. Penttilä, S. Rahaman, S. Rinta-Antila, J. Rissanen, A. Saastamoinen, J. Szerypo, C. Weber, and J. Äystö, The European Physical Journal A **48** (2012), 10.1140/epja/i2012-12046-1.

[29] G. Gräff, H. Kalinowsky, and J. Traut, Zeitschrift für Physik A: Atoms and Nuclei **297**, 35 (1980).

[30] M. König, G. Bollen, H.-J. Kluge, T. Otto, and J. Szerypo, International Journal of Mass Spectrometry and Ion Processes **142**, 95 (1995).

[31] G. Savard, S. Becker, G. Bollen, H.-J. Kluge, R. Moore, T. Otto, L. Schweikhard, H. Stolzenberg, and U. Wiess, Physics Letters A **158**, 247 (1991).

[32] M. Kretzschmar, International Journal of Mass Spectrometry **264**, 122 (2007).

[33] S. George, K. Blaum, F. Herfurth, A. Herlert, M. Kretzschmar, S. Nagy, S. Schwarz, L. Schweikhard, and C. Yazidjian, International Journal of Mass Spectrometry **264**, 110 (2007).

[34] A. Kellerbauer, K. Blaum, G. Bollen, F. Herfurth, H.-J. Kluge, M. Kuckein, E. Sauvan, C. Scheidenberger, and L. Schweikhard, The European Physical Journal D - Atomic, Molecular, Optical and Plasma Physics **22**, 53 (2003).

[35] R. T. Birge, Phys. Rev. **40**, 207 (1932).

[36] M. Vilén, D. A. Nesterenko, T. Eronen, and A. Kankainen, To be submitted (2019).

[37] D. A. Nesterenko, T. Eronen, A. Kankainen, L. Canete, A. Jokinen, I. D. Moore, H. Penttilä, S. Rinta-Antila, A. de Roubin, and M. Vilen, The European Physical Journal A **54**, 154 (2018).

[38] M. Wang, G. Audi, F. Kondev, W. Huang, S. Naimi, and X. Xu, Chinese Physics C **41**, 030003 (2017).

[39] G. Audi, F. G. Kondev, M. Wang, W. Huang, and S. Naimi, Chinese Physics C **41**, 030001 (2017).

[40] Y. Xing, K. Li, Y. Zhang, X. Zhou, M. Wang, Y. Litvinov, K. Blaum, S. Wanajo, S. Kubono, G. Martínez-Pinedo, A. Sieverding, R. Chen, P. Shuai, C. Fu, X. Yan, W. Huang, X. Xu, X. Tang, H. Xu, T. Bao, X. Chen, B. Gao, J. He, Y. Lam, H. Li, J. Liu, X. Ma, R. Mao, M. Si, M. Sun, X. Tu, Q. Wang, J. Yang, Y. Yuan, Q. Zeng, P. Zhang, X. Zhou, W. Zhan, S. Litvinov, G. Audi, T. Uesaka, Y. Yamaguchi, T. Yamaguchi,

[40] A. Ozawa, C. Fröhlich, T. Rauscher, F.-K. Thielemann, B. Sun, Y. Sun, A. Dai, and F. Xu, Physics Letters B **781**, 358 (2018).

[41] X. Tu, M. Wang, Y. Litvinov, Y. Zhang, H. Xu, Z. Sun, G. Audi, K. Blaum, C. Du, W. Huang, Z. Hu, P. Geng, S. Jin, L. Liu, Y. Liu, B. Mei, R. Mao, X. Ma, H. Suzuki, P. Shuai, Y. Sun, S. Tang, J. Wang, S. Wang, G. Xiao, X. Xu, J. Xia, J. Yang, R. Ye, T. Yamaguchi, X. Yan, Y. Yuan, Y. Yamaguchi, Y. Zang, H. Zhao, T. Zhao, X. Zhang, X. Zhou, and W. Zhan, Nucl. Instrum. Meth. Phys. Res. A **654**, 213 (2011).

[42] X. Xu, P. Zhang, P. Shuai, R. J. Chen, X. L. Yan, Y. H. Zhang, M. Wang, Y. A. Litvinov, H. S. Xu, T. Bao, X. C. Chen, H. Chen, C. Y. Fu, S. Kubono, Y. H. Lam, D. W. Liu, R. S. Mao, X. W. Ma, M. Z. Sun, X. L. Tu, Y. M. Xing, J. C. Yang, Y. J. Yuan, Q. Zeng, X. Zhou, X. H. Zhou, W. L. Zhan, S. Litvinov, K. Blaum, G. Audi, T. Uesaka, Y. Yamaguchi, T. Yamaguchi, A. Ozawa, B. H. Sun, Y. Sun, A. C. Dai, and F. R. Xu, Phys. Rev. Lett. **117**, 182503 (2016).

[43] P. Zhang, X. Xu, P. Shuai, R. Chen, X. Yan, Y. Zhang, M. Wang, Y. Litvinov, K. Blaum, H. Xu, T. Bao, X. Chen, H. Chen, C. Fu, J. He, S. Kubono, Y. Lam, D. Liu, R. Mao, X. Ma, M. Sun, X. Tu, Y. Xing, J. Yang, Y. Yuan, Q. Zeng, X. Zhou, X. Zhou, W. Zhan, S. Litvinov, G. Audi, T. Uesaka, Y. Yamaguchi, T. Yamaguchi, A. Ozawa, B. Sun, Y. Sun, and F. Xu, Phys. Lett. B **767**, 20 (2017).

[44] Y. H. Zhang, P. Zhang, X. H. Zhou, M. Wang, Y. A. Litvinov, H. S. Xu, X. Xu, P. Shuai, Y. H. Lam, R. J. Chen, X. L. Yan, T. Bao, X. C. Chen, H. Chen, C. Y. Fu, J. J. He, S. Kubono, D. W. Liu, R. S. Mao, X. W. Ma, M. Z. Sun, X. L. Tu, Y. M. Xing, Q. Zeng, X. Zhou, W. L. Zhan, S. Litvinov, K. Blaum, G. Audi, T. Uesaka, Y. Yamaguchi, T. Yamaguchi, A. Ozawa, B. H. Sun, Y. Sun, and F. R. Xu, Phys. Rev. C **98**, 014319 (2018).

[45] C. Yazidjian, G. Audi, D. Beck, K. Blaum, S. George, C. Guénaut, F. Herfurth, A. Herlert, A. Kellerbauer, H.-J. Kluge, D. Lunney, and L. Schweikhard, Phys. Rev. C **76**, 024308 (2007).

[46] S. George, G. Audi, B. Blank, K. Blaum, M. Breitenfeldt, U. Hager, F. Herfurth, A. Herlert, A. Kellerbauer, H.-J. Kluge, M. Kretzschmar, D. Lunney, R. Savreux, S. Schwarz, L. Schweikhard, and C. Yazidjian, EPL (Europhysics Letters) **82**, 50005 (2008).

[47] T. K. Nieto, J. Souin, T. Eronen, L. Audirac, J. Äystö, B. Blank, V. V. Elomaa, J. Giovinazzo, U. Hager, J. Hakala, A. Jokinen, A. Kankainen, P. Karvonen, T. Kessler, I. D. Moore, H. Penttilä, S. Rahaman, M. Reponen, S. Rinta-Antila, J. Rissanen, A. Saastamoinen, T. Sonoda, and C. Weber, Phys. Rev. C **80**, 035502 (2009).

[48] A. Kankainen, T. Eronen, D. Gorelov, J. Hakala, A. Jokinen, V. S. Kolhinen, M. Reponen, J. Rissanen, A. Saastamoinen, V. Sonnenschein, and J. Äystö, Phys. Rev. C **89**, 051302 (2014).

[49] D. A. Nesterenko, A. Kankainen, L. Canete, M. Block, D. Cox, T. Eronen, C. Fahlander, U. Forsberg, J. Gerl, P. Golubev, J. Hakala, A. Jokinen, V. S. Kolhinen, J. Koponen, N. Lalović, C. Lorenz, I. D. Moore, P. Papadakis, J. Reinikainen, S. Rinta-Antila, D. Rudolph, L. G. Sarmiento, A. Voss, and J. Äystö, J. Phys. G: Nucl. Part. Phys. **44**, 065103 (2017).

[50] A. Kankainen, V.-V. Elomaa, T. Eronen, D. Gorelov,

J. Hakala, A. Jokinen, T. Kessler, V. S. Kolhinen, I. D. Moore, S. Rahaman, M. Reponen, J. Rissanen, A. Saastamoinen, C. Weber, and J. Äystö, Phys. Rev. C **82**, 034311 (2010).

[51] A. A. Valverde, M. Brodeur, G. Bollen, M. Eibach, K. Gulyuz, A. Hamaker, C. Izzo, W.-J. Ong, D. Puentes, M. Redshaw, R. Ringle, R. Sandler, S. Schwarz, C. S. Sumithrarachchi, J. Surbrook, A. C. C. Villari, and I. T. Yandow, Phys. Rev. Lett. **120**, 032701 (2018).

[52] J. Fallis, J. A. Clark, K. S. Sharma, G. Savard, F. Buchinger, S. Caldwell, A. Chaudhuri, J. E. Crawford, C. M. Deibel, S. Gulick, A. A. Hecht, D. Lascar, J. K. P. Lee, A. F. Levand, G. Li, B. F. Lundgren, A. Parikh, S. Russell, M. Scholte-van de Vorst, N. D. Scielzo, R. E. Segel, H. Sharma, S. Sinha, M. G. Sternberg, T. Sun, I. Tanihata, J. Van Schelt, J. C. Wang, Y. Wang, C. Wrede, and Z. Zhou, Phys. Rev. C **84**, 045807 (2011).

[53] C. Guénaut, G. Audi, D. Beck, K. Blaum, G. Bollen, P. Delahaye, F. Herfurth, A. Kellerbauer, H.-J. Kluge, J. Libert, D. Lunney, S. Schwarz, L. Schweikhard, and C. Yazidjian, Phys. Rev. C **75**, 044303 (2007).

[54] P. Schury, C. Bachelet, M. Block, G. Bollen, D. A. Davies, M. Facina, C. M. Folden III, C. Guénaut, J. Huikari, E. Kwan, A. Kwiatkowski, D. J. Morrissey, R. Ringle, G. K. Pang, A. Prinke, J. Savory, H. Schatz, S. Schwarz, C. S. Sumithrarachchi, and T. Sun, Phys. Rev. C **75**, 055801 (2007).

[55] J. Savory, P. Schury, C. Bachelet, M. Block, G. Bollen, M. Facina, C. M. Folden, C. Guénaut, E. Kwan, A. A. Kwiatkowski, D. J. Morrissey, G. K. Pang, A. Prinke, R. Ringle, H. Schatz, S. Schwarz, and C. S. Sumithrarachchi, Phys. Rev. Lett. **102**, 132501 (2009).

[56] H. Herndl and B. Brown, Nuclear Physics A **627**, 35 (1997).

[57] M. Honma, T. Otsuka, T. Mizusaki, and M. Hjorth-Jensen, Phys. Rev. C **80**, 064323 (2009).

[58] B. A. Brown and A. F. Lisetskiy, (unpublished) see also endnote (28) in B. Cheal et al., Phys. Rev. Lett. 104, 252502 (2010).

[59] D. Rudolph, F. Cristancho, C. J. Gross, A. Jungclaus, K. P. Lieb, M. A. Bentley, W. Gelletly, J. Simpson, H. Grawe, J. Heese, K. H. Maier, J. Eberth, S. Skoda, J. L. Durell, B. J. Varley, D. J. Blumenthal, C. J. Lister, and S. Rastikerdar, J. Phys. G: Nucl. Part. Phys. **17**, L113 (1991).

[60] A. Odahara, Y. Gono, S. Mitarai, T. Shizuma, E. Ideguchi, J. Mukai, H. Tomura, B. J. Min, S. Suematsu, T. Kuroyanagi, K. Heiguchi, T. Komatsubara, and K. Furuno, Zeitschrift für Physik A Hadrons and Nuclei **354**, 231 (1996).

[61] A. B. Garnsworthy, P. H. Regan, S. Pietri, Y. Sun, F. R. Xu, D. Rudolph, M. Górska, L. Cáceres, Z. Podolyák, S. J. Steer, R. Hoischen, A. Heinz, F. Becker, P. Bednarczyk, P. Doornenbal, H. Geissel, J. Gerl, H. Grawe, J. Grębosz, A. Kelic, I. Kojouharov, N. Kurz, F. Montes, W. Prokopwicz, T. Saito, H. Schaffner, S. Tachenov, E. Werner-Malento, H. J. Wollersheim, G. Benzoni, B. Blank, C. Brandau, A. M. Bruce, F. Camera, W. N. Catford, I. J. Cullen, Z. Dombrádi, E. Estevez, W. Gelletly, G. Ilie, J. Jolie, G. A. Jones, A. Jungclaus, M. Kmiecik, F. G. Kondev, T. Kurtukian-Nieto, S. Lalkovski, Z. Liu, A. Maj, S. Myalski, M. Pfützner, S. Schwertel, T. Shizuma, A. J. Simons,

P. M. Walker, and O. Wieland, Physical Review C **80** (2009), 10.1103/physrevc.80.064303.

[62] R. Gross and A. Frenkel, Nucl. Phys. A **267**, 85 (1976).

[63] B. A. Brown, Phys. Rev. Lett. **111**, 162502 (2013).

[64] W. Satuła, J. Dobaczewski, and W. Nazarewicz, Phys. Rev. Lett. **81**, 3599 (1998).